2003

Corrosion Protection of Steel Using Nonanomalous Ni-Zn-P Coatings

Basker Veeraraghavan
University of South Carolina - Columbia

Bala Haran
University of South Carolina - Columbia

Swaminatha P. Kumaraguru
University of South Carolina - Columbia

Branko N. Popov
University of South Carolina - Columbia, popov@engr.sc.edu

Publication Info

Journal of the Electrochemical Society, 2003, pages B131-B139.

Publisher's link: http://dx.doi.org/10.1149/1.1556015
DOI: 10.1149/1.1556015

Journal of The Electrochemical Society, **150** (4) B131-B139 (2003)
0013-4651/2003/150(4)/B131/9/$7.00 © The Electrochemical Society, Inc.

Corrosion Protection of Steel Using Nonanomalous Ni-Zn-P Coatings

Basker Veeraraghavan,* Bala Haran, Swaminatha P. Kumaraguru,* and Branko Popov**,z**

Center for Electrochemical Engineering, Department of Chemical Engineering, University of South Carolina, Columbia, South Carolina 29208, USA

A novel technique for obtaining nonanomalous Ni-Zn-P coatings with high Ni content (74 wt % as compared to 15-20 wt % in the conventional plating method) has been developed. These coatings show promise as a replacement for Cd in sacrificially protecting steel. Ni-Zn-P coatings were deposited using an electroless method from a solution containing $NiSO_4$, complexing agent and ammonium chloride. Varying the concentration of $ZnSO_4$ in the bath controls the final amount of Zn in the deposit. The Zn content in the coating was optimized based on the corrosion resistance of the final deposit. Coatings with 16.2 wt % Zn were found to display a potential of −0.652 V *vs.* SCE that is more electronegative to steel and hence can be used as a sacrificial coating for the protection of steel. Deposition parameters like pH and temperature have been optimized based on composition of the coating and the surface morphology. Corrosion studies in corroding media show that Ni-Zn-P coatings obtained using the electroless method show a higher barrier resistance and better stability as compared to cadmium coatings.
 [DOI: 10.1149/1.1556015]

Manuscript submitted June 13, 2002; revised manuscript received September 26, 2002. Available electronically February 28, 2003.

Cadmium has been extensively used as a barrier coating for steel in aerospace, electrical, and fastener industries owing to its excellent corrosion resistance and other engineering properties.[1] Plating of cadmium poses considerable challenges, due to the toxicity of the metal and its salts.[2] Further, during cadmium deposition, huge amounts of hydrogen are introduced into the substrate, thus making the substrate susceptible to hydrogen embrittlement failure.[3] Hence, for environmental and hydrogen embrittlement reasons, alternate coatings to cadmium are being actively explored. The most commonly used sacrificial coating in place of cadmium is zinc and its alloys. Zinc, by the virtue of its low standard electrode potential ($E_0 = -0.76$ V *vs.* NHE), makes it suitable to act as a sacrificial coating on steel.[4] The difference in the potentials of the coating and the substrate act as the driving force for the corrosion of the sacrificial coating under corroding conditions. Owing to the huge difference in electronegativities of Zn and Fe, rapid dissolution of Zn happens under corroding conditions. The problem of accelerated corrosion of Zn has been mitigated to some extent by alloying it with another metal that will bring the standard electrode potential of the alloy much closer to the substrate metal. It has been shown that zinc, when alloyed with metals like Ni, Fe, and Co, provides improved corrosion resistance to steel substrates.[5] Of these alloys, Zn-Ni has been suggested as the replacement for cadmium coatings in view of their corrosion resistance, better formability, and improved weldability.[6,7]

The deposition of such alloys has been shown to be anomalous in nature. Although Ni is more noble than Zn, the codeposition of these metals results in a higher amount of Zn in the final deposit. Since the deposit still has a higher amount of Zn, the rate of dissolution of these alloys remains high under corroding conditions. The mechanism for this preferential deposition has been discussed extensively in the literature.[8,9] Several researchers have attempted to decrease the anomaly of the deposit because an increase in the Ni composition would lead to more anodic potentials, which in turn will reduce the driving force for the galvanic corrosion. Such attempts have focused on the use of inert species in the bath or development of an alternate ternary alloy.[10-13] In our previous study, nonyl phenyl polyethylene oxide (NPPO) was found to inhibit zinc electrodeposition and to act as a leveling agent.[10] Zhou *et al.* have studied the effects of the addition of tin on the anomalous deposition of Zn-Ni alloys.[11] The amount of Ni in the deposit was found to increase marginally from 6 to 8 wt % with small inclusions of tin. However, the observed small increase in Ni content of the alloy did not improve the barrier properties. We have also found that the codeposition of phosphorus along with Zn-Ni increases the corrosion resistance[12] and hydrogen permeation resistance[13] of the coating. We have also shown that the addition of small amounts of Cd to the Zn-Ni plating bath increases the barrier properties and hydrogen permeation resistance properties of the ternary alloy coating in comparison to Zn-Ni alloys.[14] However, Cd addition in the bath is undesirable owing to the stringent regulations involved in the disposal of that metal and its salts. However, in all these cases, the amount of zinc in the final deposit still varies between 70-90% and hence their rate of dissolution remains high.

Autocatalytic reduction of metals and alloys offers an attractive and alternate method of increasing the amount of Ni in the final deposit. Electroless deposition has been used to form a thin and uniform Ni-Zn-P film from both sulfate and chloride baths. Previous efforts have shown that Ni-Zn-P plating follows normal deposition with high Ni content (80-90%).[15-17] However, in these cases, the amount of Zn remains low (~10 wt %) and hence the potential (−476 mV *vs.* SCE) is more positive to steel (−590 mV *vs.* SCE). Thus these deposits, although offering excellent corrosion resistance, could not be used as a sacrificial coating for steel. In our present study, our objective is to enhance the zinc content in the alloy and thereby ensure that the coating will exhibit sacrificial properties while providing extended life in corroding media. The corrosion characteristics of these newly developed composite coatings have been compared to that of cadmium.

Experimental

Sample preparation.—Plating and subsequent corrosion studies were done on low carbon cold-rolled steel foils of thickness 0.5 mm and area 25 × 25 mm. Initially, the steel sample was mechanically polished with successively finer grades of emery paper. The samples were then degreased with alcohol and rinsed with deionized water. Next, the samples were treated in 10% (v/v) H_2SO_4 solution for 1 min to remove any adherent oxide layer present on the surface. Finally, the samples were again washed in deionized water. This procedure was repeated until a clean and smooth surface was obtained.

Electrolyte preparation and deposition.—Ni-Zn-P composites were prepared from a bath containing 35 g/L $NiSO_4$, complexing agent and 50 g/L NH_4Cl. Sodium hypophosphite was used as a reducing agent for the autocatalytic process and as a source of P in the final deposit. Steel foil prepared as mentioned above was used as

* Electrochemical Society Student Memeber.
** Electrochemical Society Active Member.
z E-mail: popov@engr.sc.edu

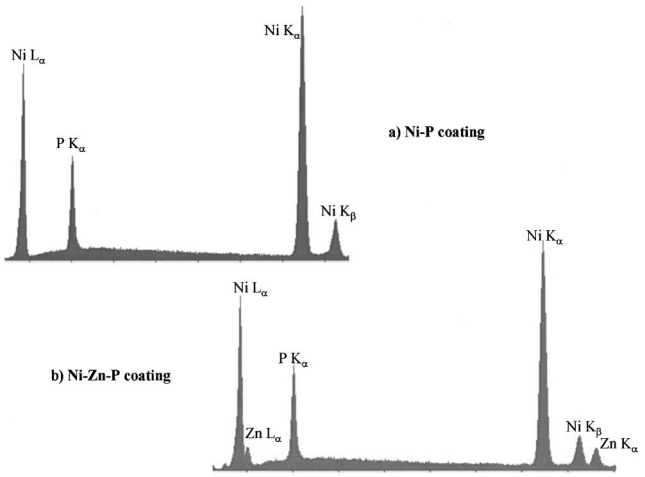

Figure 1. EDAX analysis on Ni-P and Ni-Zn-P (prepared with 5 g/L $ZnSO_4 \cdot 7H_2O$). New peaks corresponding to Zn Lα and Zn Kα are seen in the case of Ni-Zn-P coatings.

the substrate. Ni-Zn-P coatings with different amounts of Zn were obtained by varying the amount of $ZnSO_4 \cdot 7H_2O$ in the bath. The deposition was carried out at 85°C unless otherwise mentioned. The time of deposition was kept constant at 1 h in all the cases. The pH was maintained at 10.5 during the deposition. All solutions were prepared with analytical grade reagents (obtained from Sigma-Aldrich) and triply distilled water.

Material characterization.—Energy dispersive analysis using X-rays (EDAX) was used to analyze the distribution of the elements in the final deposit. To ensure accuracy of the element distributions, EDAX analysis was done at several points on the surface of the substrate. The accuracy of the measurements for the equipment used was rated as ±0.1 wt %. The surface morphology and the microstructure of the coating were analyzed using scanning electron microscopy (SEM) with the help of Hitachi S-2500 Delta scanning electron microscope. The thickness of the specimens was measured using cross-sectional SEM analysis. The thickness measurements were done in accordance with ASTM standard B659[18] by preparing a cross section of the samples in a low temperature mounting procedure (as prescribed for low temperature alloys like Ni-P).

Electrochemical characterization.—A variety of electrochemical techniques including linear and Tafel polarization were used to evaluate the barrier resistance properties of the coating. Since chemical dissolution of Zn occurs in both acidic and alkaline media, corrosion testing was performed in 71 g/L Na_2SO_4 and 30.5 g/L H_3BO_3 solution at pH 7.0. The electrochemical characterization was done using an EG&G PAR model 273A potentiostat/galvanostat interfaced with a computer and a three-electrode setup. The steel substrate with the coating was used as the working electrode, and a platinum mesh was used as the counter electrode. A standard calomel electrode (SCE) was used as the reference electrode. All potentials in this study are referenced to the SCE.

Results and Discussion

Figure 1 shows the EDAX analysis of the deposit with and without the presence of Zn ions. In the absence of Zn ions, the deposit contains peaks that correspond to Ni Lα, Ni Kα, Ni Kβ, and P Kα energy lines. However, when Zn ions are added in the solution, EDAX analysis shows new peaks for Zn Kα and Zn Lα lines, thus confirming the inclusion of Zn in the final deposit. The mechanism for electroless Ni-P deposition using sodium hypophosphite as the reducing agent has been well-established in the literature. The deposition mechanism is best explained by the mixed potential theory.[19] According to this theory, the simultaneous oxidation of hypophosphite and the reduction of nickel ions occur on a suitable substrate at a potential that is between the half-cell potentials of the individual reactions. The oxidation of hyphosphite species is given by the equation[20]

$$H_2PO_2^- + H_2O \rightarrow 2H^+ + H_2PO_3^- + 2e^- \qquad E_0 = -0.75 \text{ V } vs. \text{ SCE} \qquad [1]$$

The reduction of nickel ion occurs according to the reaction[21]

$$Ni^{2+} + 2e^- \rightarrow Ni \quad E_0 = -0.53 \text{ V } vs. \text{ SCE} \qquad [2]$$

The reduction of Ni ions is accompanied by the hydrogen evolution reaction[21]

$$2H^+ + 2e^- \rightarrow H_2 \quad E_0 = -0.28 \text{ V } vs. \text{ SCE} \qquad [3]$$

Thus, the mixed potential theory provides satisfactory explanations for the simultaneous oxidation of hypophosphite and reduction of nickel ions accompanied by hydrogen discharge. However, when Zn is added to the bath, codeposition of Zn occurs along with Ni-P deposition. The reduction of Zn proceeds according to the following reaction[21]

$$Zn^{2+} + 2e^- \rightarrow Zn \quad E_0 = -1.043 \text{ V } vs. \text{ SCE} \qquad [4]$$

Since Zn ion reduction occurs at a potential much more negative than the oxidation of hypophosphite, the mixed-potential theory fails to explain the inclusion of Zn in the deposit. To confirm this, a bath was prepared without Ni, the other constituents being kept constant to do electroless plating of Zn. No deposition was observed in this case. This shows that the Zn inclusion in the deposit occurs through other means. A plausible explanation for the deposition is inclusion of Zn during Ni deposition. It has been previously observed[22] that Zn is codeposited during potentiostatic deposition from a Zn-Ni bath in the potential range −0.7 to −0.9 V *vs.* Ag/AgCl. This produces a nonanomalous coating with 70% Ni.[22] Due to thermodynamic considerations Zn deposition through Zn^{2+} ion reduction is not possible at these potentials. Miranda *et al.*[23] have observed that the formation of Ni-rich phase in Zn-Ni alloy occurs at low potentials through the formation and subsequent reduction of $ZnNi_{ad}^+$ species. This observation tends to suggest that a similar phenomenon occurs in the electroless deposition of Ni-Zn-P. The present paper is focused on developing nonanomalous Ni-Zn-P deposits and optimizing the deposition process.

Effect of Zn^{2+} ions on the coating composition.—The effect of Zn^{2+} ions on the rate of the alloy deposition and the amount of Zn in the final deposit was studied by varying the amount of $ZnSO_4$ added to the bath from 5 to 20 g/L. Leukonis *et al.*[24] have observed that Zn^{2+} ions (apart from Ag^+ and Cd^{2+}) act as an inhibitor for the electroless Ni-P process. Hence, it can be expected that addition of Zn will reduce the rate of alloy deposition. The thickness of the obtained deposits was checked using cross-sectional SEM analysis. Figure 2 shows the cross-sectional SEM pictures of Ni-P and Ni-Zn-P coatings when 5 g/L $ZnSO_4$ is added in the bath. The figure shows a decrease in the thickness of the final coating. The thickness decreases from 15.6 μm (for Ni-P coating) to 10.2 μm (for Ni-Zn-P coating). Figure 3 shows the effect of $ZnSO_4 \cdot 7H_2O$ bath concentration on the deposition rate and the deposit thickness. As seen from the plot, the deposition rate and hence the thickness decrease is in direct proportion to the amount of Zn added in the bath. This is in agreement with the results of Valova *et al.*,[16] who observed a similar decrease in the deposition rate with an increase in the amount of Zn in the bath.

As our primary objective is to increase the amount of Zn content in the final deposit, it is essential to estimate the amount of Zn in the final deposit. EDAX analysis was used for this purpose. Figure 4 shows the distribution of Zn, Ni, and P in the coating as a function of $ZnSO_4$ added in the bath. It can be seen from the plot that the Zn

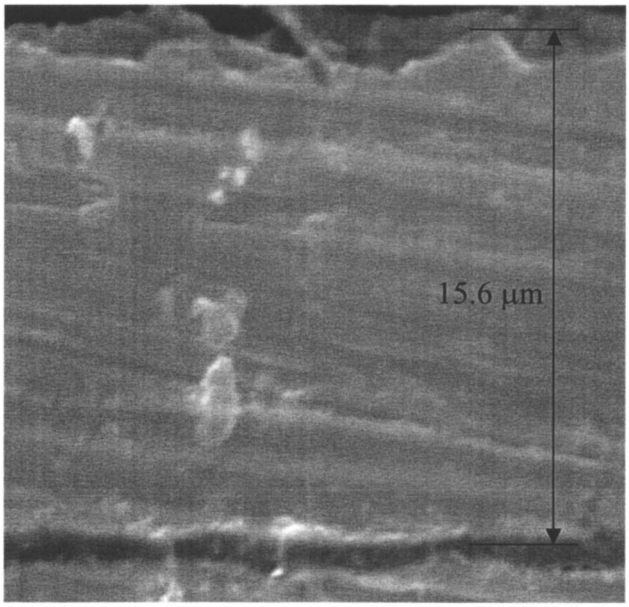

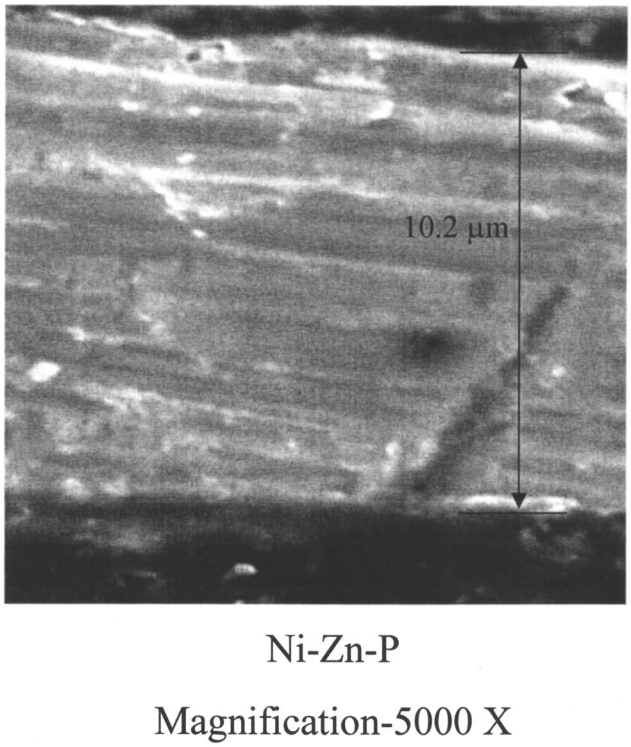

Figure 2. Cross-sectional SEM pictures of the Ni-P and Ni-Zn-P coatings (prepared with 5 g/L $ZnSO_4 \cdot 7H_2O$) for determining the thickness of the coatings.

content in the deposit increases from 10.8 wt % in the case of 5 g/L $ZnSO_4$ to 17.9 wt % in the case of 20 g/L $ZnSO_4$. The amount of Ni decreases from 78.9 to 72.1 wt % with increasing $ZnSO_4$ concentration in the bath. The P content in the deposit remains unaffected with the increase in Zn concentration. Previous results by Bouanani *et al.*[15] and Schlesinger *et al.*[17] show that the amount of P in the deposit decreases when Zn is added to the electroless Ni-P bath. This result shows that the deposition mechanism for P is different in our case. There are different mechanisms available for P liberation through the oxidation of hypophosphite depending on the bath pH. One of them is the production of P through nascent hydrogen production (called the indirect mechanism) as proposed by Ratzker *et al.*[25] Their mechanism has been accepted for the case of lower P inclusion in the electroless deposits, whereas the direct P mechanism is usually cited for high P content.[19] Earlier works on Ni-Zn-P[15,17] suggest a change in hypophosphite oxidation from direct to indirect mechanism, when Zn^{2+} is added to the bath. Further studies are being carried out in order to understand the mechanism of hypophosphite oxidation in our case.

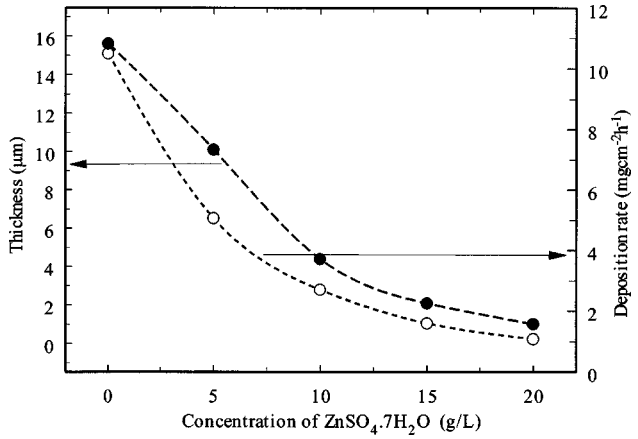

Figure 3. Variation in the deposition rate and the thickness of the coatings obtained as a function of $ZnSO_4 \cdot 7H_2O$ concentration in the bath.

In our case, it is seen that the rate decreases and Zn content increases with an increase in $ZnSO_4$ concentration in the bath. Hence, it is essential to strike a balance between the amount of Zn in the deposit while allowing the deposition to proceed at acceptable rates. In order to evaluate the optimal Zn concentration in the bath, the potential and the corrosion resistance of the samples were evaluated in the next set of studies.

To check the suitability of the coating as a sacrificial layer, the rest potentials of the coatings were tested 71 g/L Na_2SO_4 + 30.5 g/L H_3BO_3 solution at pH 7.0. Figure 5 shows the rest potential of the coatings with various amounts of Zn. The steel substrate exhibits a potential of −0.590 V *vs.* SCE. It can be seen from the graph that an increase in Zn content leads to a shift in the

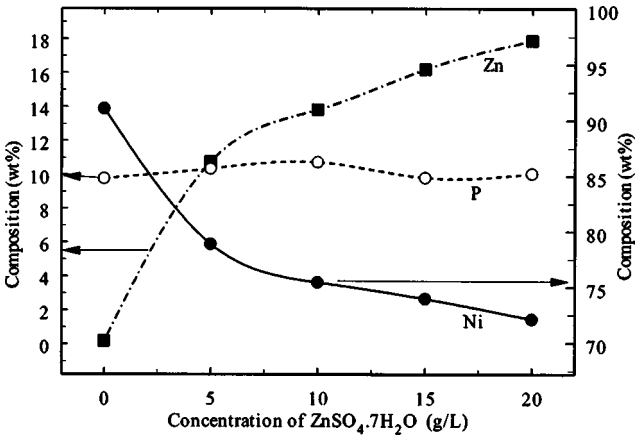

Figure 4. Change in the Ni, Zn, and P content in the deposit as a function of $ZnSO_4 \cdot 7H_2O$ concentration added in the bath.

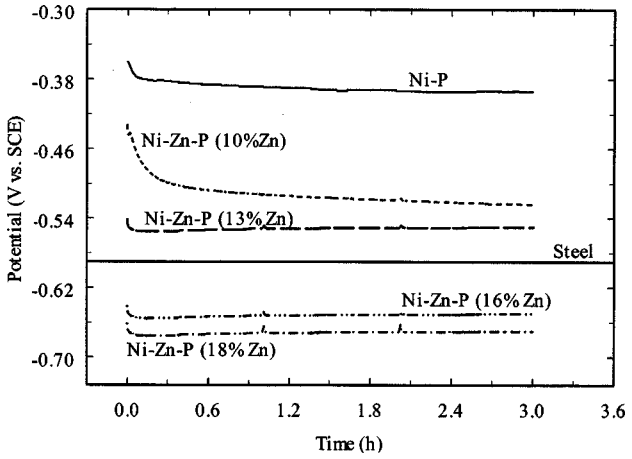

Figure 5. Rest potentials of the Ni-Zn-P deposits as a function of Zn content in the coatings.

potential to a more negative value. Coatings with no Zn show a rest potential of −0.4 V *vs.* SCE. Increase in the Zn content to 17.9 wt % results in the potential being shifted to −0.663 V *vs.* SCE. The graph also shows that the potential of the coating with 16.2 wt % Zn displays a potential (−0.652 V *vs.* SCE) that is sufficiently negative to the steel substrate. Coatings with 13.8 wt % Zn and 10.8 wt % Zn have potentials more positive to steel and hence cannot act as a sacrificial coating. As the Zn and Ni content in the deposits vary, it can be expected that the coatings containing a higher amount of Ni to possess a higher corrosion resistance. Hence, Tafel studies were done to evaluate the corrosion resistance of the coatings.

Tafel polarization was performed to evaluate the corrosion rates of the coatings with different Zn contents. The Tafel studies were carried out by scanning the potential from −200 to 200 mV with respect to the corrosion potential. The resultant Tafel plots are shown in Fig. 6. As shown in the plot, the corrosion current of the deposits increases with the increase in the amount of Zn. The increased corrosion rate in the alloyed coatings with higher amounts of Zn, is due to the lowering of the corrosion potential and to an activation of the anodic dissolution of the metal coating due to zinc alloying. However, it has to be noted that the corrosion potential shifts to a more negative value (as already seen in the rest potential studies) with an increase in Zn. Table I summarizes the corrosion

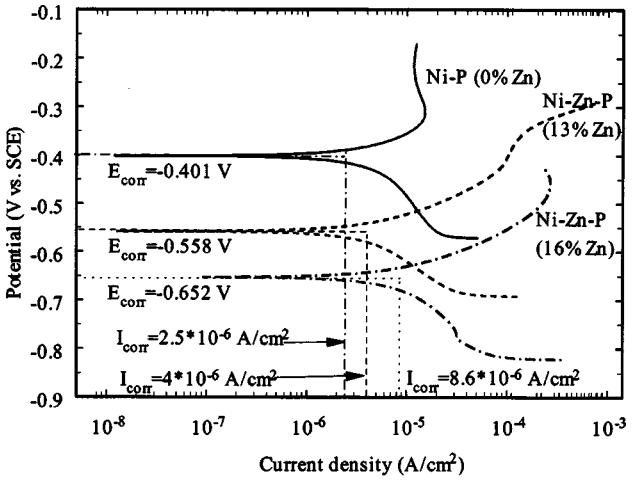

Figure 6. Tafel analysis of the Ni-Zn-P coatings as a function of Zn content in the final deposit. The corrosion potential becomes more electronegative as more Zn is included in the deposit.

Table I. Variation in corrosion potential and corrosion current density as a function of Zn content in the coatings.

Zn content in the deposit (wt %)	Corrosion potential E_{corr} (V *vs.* SCE)	Corrosion current density I_{corr} (A/cm^2)
0	−0.401	2.5×10^{-6}
10.8	−0.500	3.2×10^{-6}
13.8	−0.558	4.0×10^{-6}
16.2	−0.652	8.6×10^{-6}
17.9	−0.663	1.2×10^{-5}

potential and the corrosion rate of the coating as a function of Zn content in the deposit. Even though the corrosion current density increases from 2.5 μA/cm^2 (for Ni-P) to 8.6 μA/cm^2 (for 16% Zn-74% Ni-10% P), the corrosion potential becomes more electronegative to steel. From the rest potential and Tafel polarization studies, the optimized Zn content in the deposit is seen to be 16.2 wt % obtained at a $ZnSO_4$ concentration of 15 g/L in the bath. Hence, the rest of the depositions were carried out at the optimized $ZnSO_4$ concentration of 15 g/L.

Effect of pH on the coating composition.—Another critical parameter that can affect the composition of the coating is the pH of the deposition bath. A complete analysis of the equilibrium reactions between the various species in the bath is necessary to identify the optimal pH of deposition. In order to accomplish this, material balances coupled with various equilibrium reactions and electroneutrality conditions was carried out to elucidate the change in the equilibrium concentration of the various electroactive species in the bath. The governing equations and the computational details are summarized in the Appendix. As the pH increases, the concentration of the bivalent ions decreases with the increase in pH. According to Pourbaix,[26] both Zn^{2+} and Ni^{2+} ions will precipitate as $Zn(OH)_2$ and $Ni(OH)_2$, respectively, at pH values greater than 7.0. For the deposition to be carried out in alkaline conditions, use of complexing agents is necessary to prevent the metal ions from spontaneous precipitation. For this purpose, sodium citrate and ammonium chloride have been used in the bath. In the presence of ammonia, the following complex ions are formed

$$Zn^{2+} + 2\ OH^- \rightarrow Zn(OH)_2 \quad [5]$$

$$Zn(OH)_2 + 4NH_3 \rightarrow Zn(NH_3)_4^{2+} + 2\ OH^- \quad [6]$$

$$Ni^{2+} + 2\ OH^- \rightarrow Ni(OH)_2 \quad [7]$$

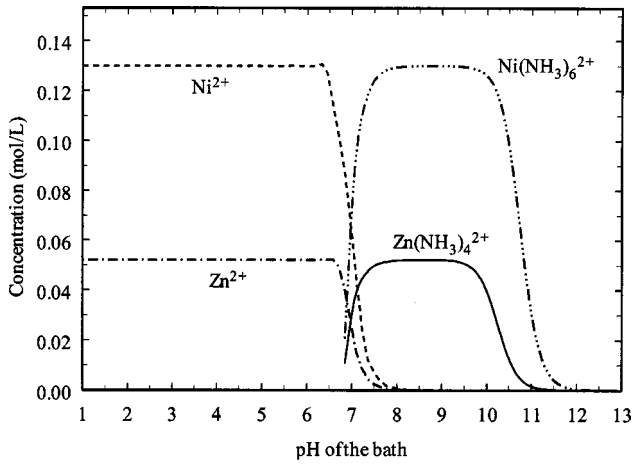

Figure 7. Equilibrium concentrations of the different electroactive species present as a function of bath pH.

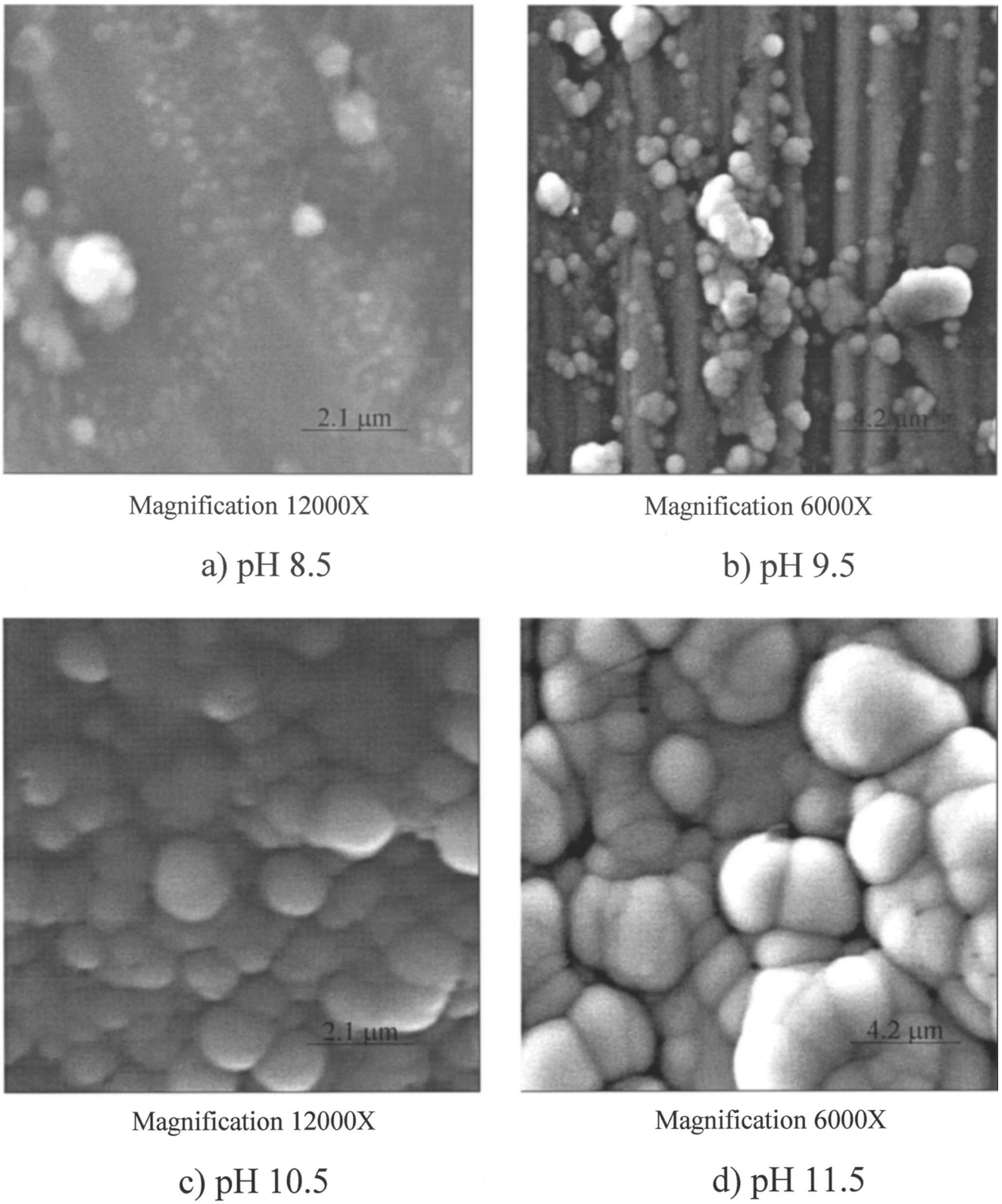

Figure 8. SEM pictures of Ni-Zn-P coatings prepared as a function of bath pH (a, top left) 8.5, (b, top right) 9.5, (c, bottom left) 10.5, and (d, bottom right) 11.5. The $ZnSO_4$ concentration is 15 g/L, and the bath temperature is 85°C.

$$Ni(OH)_2 + 6NH_3 \rightarrow Ni(NH_3)_6^{2+} + 2\ OH^- \quad [8]$$

$$Zn(NH_3)_4^{2+} + 2e^- \rightarrow Zn + 4NH_3 \quad [9]$$

Ammonia is released through the following redox reactions

$$Ni(NH_3)_6^{2+} + 2e^- \rightarrow Ni + 6NH_3 \quad [10]$$

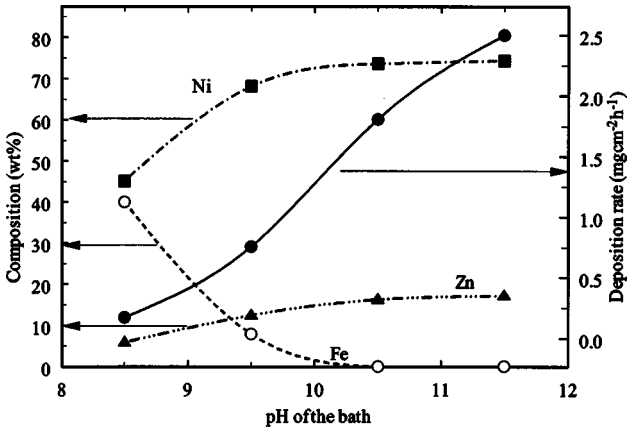

Figure 9. Variation in the rate of deposition and Ni, Zn, and Fe content as a function of bath pH.

The equilibrium concentrations of the various species as a function of bath pH are shown in Fig. 7. As seen from the plot, the ratio of the concentrations of the complexed Zn and Ni ions remains constant from pH 7.5 to 9.5. However, above pH 9.5, the concentration of the complexed ions changes rapidly and beyond pH 11.5, the complexed ions precipitate as their respective hydroxides. The decrease in complex Ni ion concentration is much larger than the decrease in complexed Zn ion concentration. This leads to an increase in the Zn/Ni ion ratio in the pH range 9.5 to 11.5. Hence the change in pH of the bath can be expected to increase the amount of Zn in the deposit. Since higher Zn ion concentration in the bath lowers the deposition rates, the drop in the complexed Zn ion concentration (in the pH range 9.5-11.5) will play a crucial role in determining the deposition rate.

To understand the effect of pH, experiments were done at four different pHs in the range 8.5-11.5. Increasing the pH beyond 11.5, results in the spontaneous precipitation of the bath. This result is consistent with the findings in the pH concentration diagram as shown in Fig. 7. Figure 8 shows the morphology of the coatings prepared at different pHs. The SEM pictures show that the depositions carried out at pH values lower than 10.5 gives rise to coatings that do not cover the substrate surface completely. The SEM pictures show that the deposition at pH 10.5 results in the coating of uniform layers of spherical particles across the entire surface. With the increase in pH to 11.5, the deposits tend to agglomerate. The surface also shows the existence of cracks on the surface that will undermine the performance of the coating in corroding media.

EDAX analysis was done to determine the deposit constituents. Figure 9 shows the effect of pH on the rate of deposition and the composition of the coating deposited at 85°C and in the presence of 15 g/L $ZnSO_4$ in the bath. Below pH 8.5, no deposition occurs on the surface. The rate of deposition increases linearly with an increase in pH. It is also seen that a high percentage of Fe is detected in the case of pH 8.5 and 9.5. The thickness of the coating was measured by both cross-sectional SEM analysis and using the weight gain method. It is seen that deposits obtained at pH 8.5 and 9.5 have thicknesses of less than 1 μm. EDAX analysis results in detecting elemental distribution to a depth of 1 μm. If the coating thickness is less than 1 μm, the underlying substrate constituents are also detected. As seen in Fig. 8a and b, the surface is not completely covered with the coating for deposits obtained at pH 8.5 and 9.5, and this could be the reason for detecting Fe. However, with an increase in pH, the Fe content decreases and reaches a value of <0.1 wt % at pH 10.5. The change in the composition of the coating is negligible after a pH of 10.5, as seen from Zn and Ni content at pH 10.5 and 11.5. Since the composition of the coating remains the same after a pH of 10.5, use of pH 11.5 might look attractive superficially for the benefit of increased rate (as seen in Fig. 9).

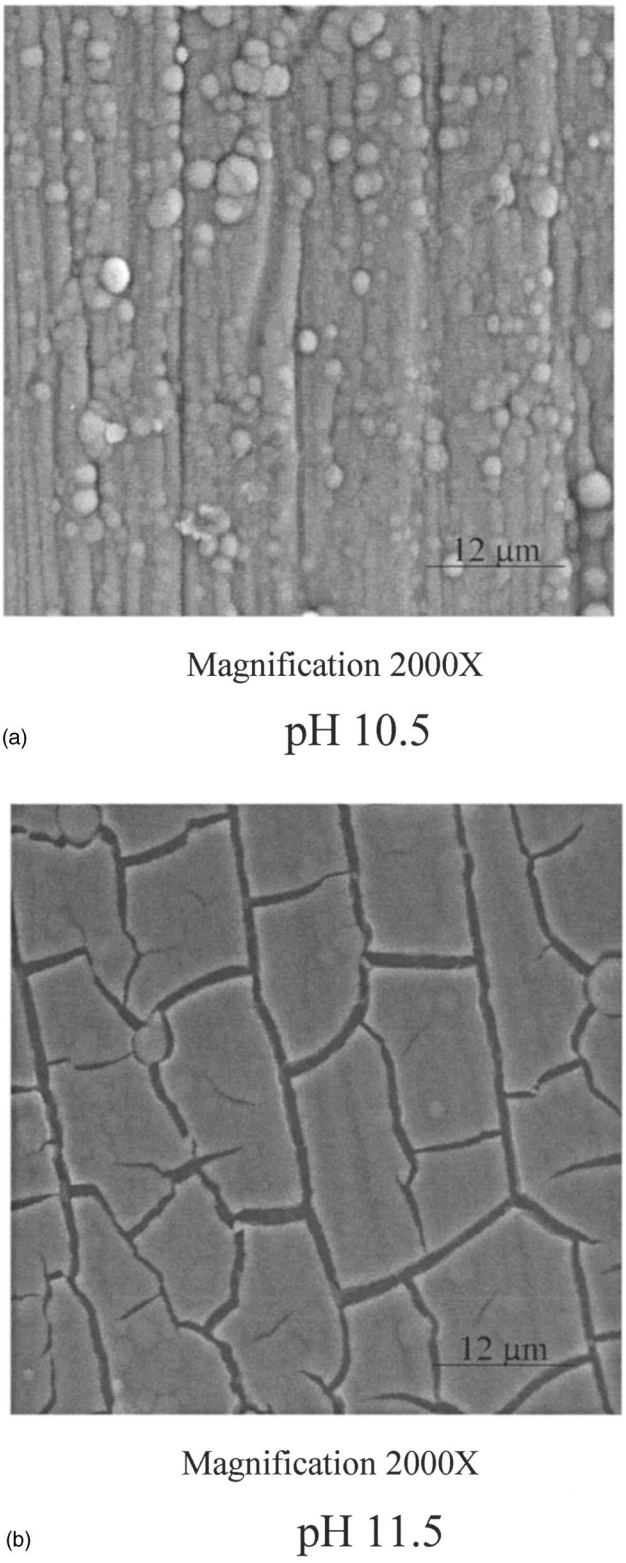

Figure 10. SEM pictures for deposits prepared at pH 10.5 (a) and 11.5 (b) after immersing them in 71 g/L Na_2SO_4 and 30.5 g/L H_3BO_3 (pH 7.0) for a day. Coatings prepared at pH 11.5 show excessive cracking.

However, the presence of cracks on the coating surface discourages the use of pH higher than 10.5. According to the literature,[16] cracks are developed in Ni-Zn-P coatings because of internal strain developed in the coatings due to incorporation of zinc in the alloy formation. Hence, the extent of crack formation is directly dependant on

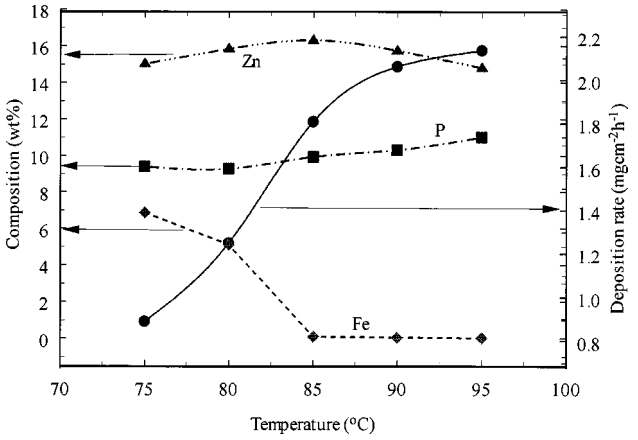

Figure 11. Variations in the rate of deposition and Zn, P, and Fe contents as a function of bath temperature.

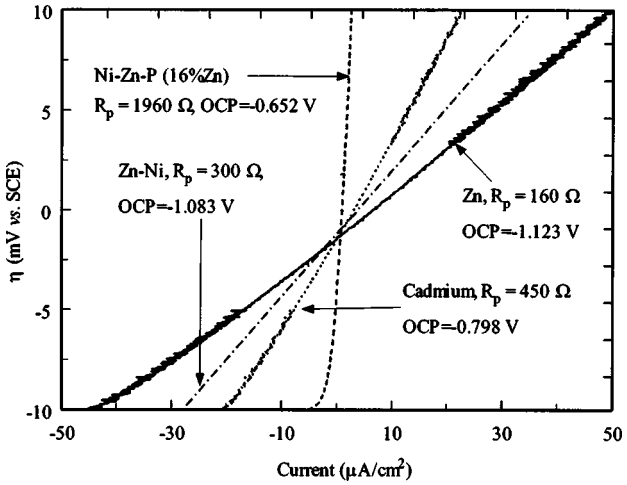

Figure 12. Linear polarization plots for the various sacrificial coatings as compared with optimized Ni-Zn-P (16.2 wt % Zn) coating. The graph shows a four-times increase in the polarization resistance for Ni-Zn-P coating as compared to Cd coating.

the rate of deposition. At pH 11.5, the rate of deposition as well as the amount of zinc in the deposit increases. As a result of larger zinc deposition at a higher rate, cracks are developed for coatings deposited at pH 11.5.

In order to confirm this, panels deposited at pH 10.5 and 11.5 were kept in 71 g/L Na_2SO_4 and 30.5 g/L H_3BO_3 (pH 7.0) for a day. SEM analysis was subsequently done to see the change in the surface morphology of the deposits due to corrosion. These results are shown in Fig. 10. Deposits obtained at pH 11.5 exhibit large cracks on their surface. Miranda *et al.*[27] have observed that the better corrosion properties exhibited by electrodeposited Zn-Ni alloys is due to the crack formation during the corrosion process. Exposure to corrosive environments will lead to enhancement of crack structure. According to Miranda *et al.*[27] Ni enrichment is seen in Zn-Ni alloys subjected to corrosion studies due to sacrificial dissolution of Zn from the deposit. Similar results can be expected from our coatings also, especially those prepared at pH 11.5. However, large cracks present initially will lead to higher crack growth and faster dissolution of Zn. To avoid this we optimized the deposition pH at 10.5. Comparison of Fig. 10a and b reveals that deposits at pH 10.5 exhibit fewer cracks and a less porous structure than coatings obtained at pH 11.5. The barrier properties of the coating obtained at pH 10.5 will ensure a long protective life for the substrate. Hence the bath pH was optimized at a value of 10.5.

Effect of temperature on the coating composition.—Maintaining the temperature at an optimal value is a critical factor in the successful operation of the electroless coatings. To study the effect of temperature on the electroless process, the deposition was carried out at different temperatures while holding the pH (10.5) and $ZnSO_4$ concentration (15 g/L) constant. Figure 11 shows the effect of temperature on the rate of deposition and the alloy composition. The most readily observed result is the increase in the rate of deposition with an increase in temperature. This is to be expected, since a rise in temperature increases the activation for the deposition process. At 75°C, the deposit does not cover the surface completely and there is still some Fe that is being exposed. With an increase in temperature to 85°C, no Fe is seen in the EDAX analysis. Beyond 85°C, no significant change in the deposition rate or the coating composition is seen. Hence, the bath temperature was optimized at 85°C.

Performance comparison with various sacrificial coatings.—As the whole endeavor of this work is to develop a sacrificial coating that can replace cadmium coatings, it is critical to compare the performance of the developed coating to cadmium and other sacrificial coatings. The coatings that have been chosen for comparison in this study are zinc, zinc-nickel, and cadmium, because these are the most commonly used sacrificial coatings for the protection of steel. Ni-Zn-P with 16.2 wt % Zn was chosen as the optimal Zn content alloy based on rest potential and Tafel studies. The thicknesses of the various coatings were approximately 2 μm for these comparison studies. The deposit thickness was estimated by dividing the weight of a unit area with the average density of the alloy.

Linear polarization studies.—Linear polarization studies were carried out to find the polarization resistances of the various coatings. The potential was swept from −10 to +10 mV *vs.* E_{corr} at a scan rate of 0.5 mV/s. The resulting graphs of overpotential *vs.* current density for the different coatings are shown in Fig. 12. The slope of these lines yields the value of the polarization resistance. The low polarization resistance for the Zn and Zn-Ni alloy coatings show that the corrosion rates for these coatings are much higher than Ni-Zn-P coatings. Table II shows the composition of the various coatings that have been chosen for comparison along with the E_{corr} values and corrosion rates. The corrosion rates have been calculated using the polarization resistance found from the linear polarization technique. We can see from the table that the corrosion rate for the electroless Ni-Zn-P (16% Zn) coatings is five times lower than Cd coatings. These studies show that the electroless Ni-Zn-P coating possesses superior corrosion characteristics as compared to the other sacrificial coatings.

Film dissolution studies.—In order to check the stability of the different coatings in corroding media, a known surface area of the coated samples was immersed in the corroding media and the open-circuit potential (ocp) was continuously monitored as a function of time. Figure 13a shows the plot of the E_{corr} values of the various coatings as a function of time. As time passes, all the coatings dissolve in the corrosion media due to their sacrificial nature. The rate of dissolution will depend on the potential difference between the substrate and the coating. The greater the potential difference, the

Table II. Comparison of corrosion potential and corrosion rates for different sacrificial coatings.

Coating	E_{corr} (V *vs.* SCE)	I_{corr} (A/cm^2)	Corrosion rate ($\times 10^{-10}$ cm/s)
Zn	−1.123	1.5×10^{-3}	39.4
94.6% Zn-5.4% Ni	−1.083	3.8×10^{-4}	17.7
Cd	−0.798	4.0×10^{-5}	17.2
74% Ni-16.2% Zn-9.8% P	−0.652	8.6×10^{-6}	3.3

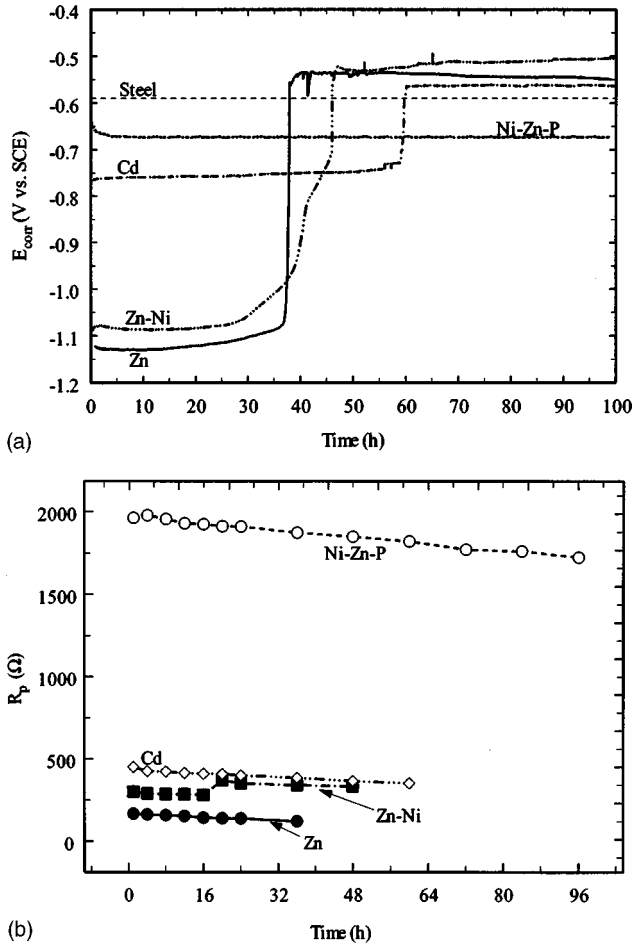

Figure 13. (a) E_{corr} *vs.* time plot for the various alloy coatings (thickness 2 μm) immersed in 71 g/L Na_2SO_4 and 30.5 g/L H_3BO_3 (pH 7.0). (b) Plot of polarization resistance *vs.* time for the various sacrificial coatings in 71 g/L Na_2SO_4 and 30.5 g/L H_3BO_3 (pH 7.0).

less time is taken for the coating to dissolve. The change in the potential to the substrate potential will give an indication of the complete dissolution of the coating. From the plot, it is seen that Zn dissolves the fastest. The potential directly jumps from −1.123 to −0.560 V *vs.* SCE, thus suggesting that Zn is present in its elemental form in the deposit. However, in the case of the Zn-Ni alloy, there are several stages of dissolution according to the various phases present in the alloy. Zn-Ni alloys deposit in several phases: (*i*) a Zn-rich phase called the eta (η) phase (E_{corr} = −1.050 V *vs.* SCE) and (*ii*) an intermediate gamma (γ) phase (E_{corr} = −0.780 V *vs.* SCE).[14] The rest potential of the Zn-Ni alloy shows the dissolution of these phases at their respective potentials, the Zn-rich η phase followed by the dissolution of the γ phase. However, the time for dissolution for the Zn-Ni alloy is longer than the sample coated with Zn, which is due to the higher corrosion resistance of the Zn-Ni alloy. Ni-Zn-P coatings last longer than Cd, Zn, and Zn-Ni coatings. The potential of the coating does not change for the time period in which these tests were carried out. The primary reason for this prolonged corrosion resistance is the low potential difference between the coating (−0.652 V *vs.* SCE) and the substrate (−0.590 V *vs.* SCE). Figure 13b shows the plot of the polarization resistance values as a function of time for the various coatings for the same time period shown in the potential studies. The corrosion resistances of the other coatings were smaller than Ni-Zn-P for the entire period of study. The Zn and Cd coating shows an almost constant resistance value till failure due to the presence of a

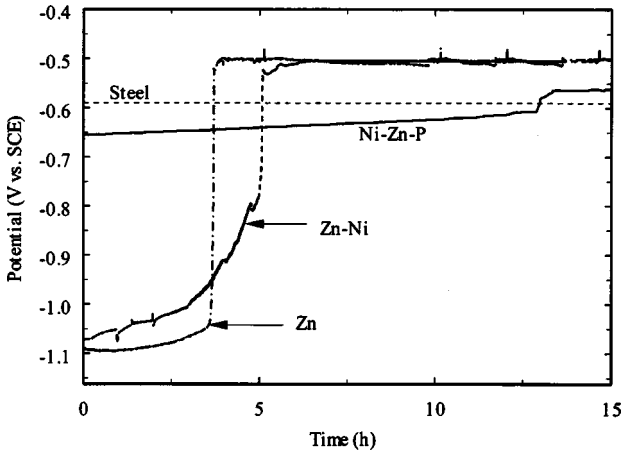

Figure 14. Corrosion potential for the various alloy coatings (thickness 2 μm) as a function of time immersed in 3.5 wt % NaCl solution.

single element. However, the resistance of the Zn-Ni alloy increased slightly with time due to the depletion of the Zn-rich η phase. Since the γ phase is known to deposit in thin layers, this, too, dissolves rapidly. However, the resistance of the Ni-Zn-P alloy remained practically constant for the period of this test, thus proving the superior corrosion characteristics of this coating.

In order to check the galvanic compatibility of the Ni-Zn-P coatings with the steel substrate, we performed thin film (2 μm thick) dissolution studies in aggressive marine environment (3.5 wt % NaCl) as suggested in Miranda *et al.*[27] Electrodeposited Zn and Zn-Ni coatings were also checked for comparison and the potential of these coatings were monitored as a function of time. These results have been summarized in Fig. 14. The results showed that the new Ni-Zn-P coatings exhibit longer life than traditional Zn and Zn-Ni coatings. The potential of the Ni-Zn-P alloys reach that of the steel substrate in about 14 h, thus providing confirmation of the alloy's ability to provide cathodic protection to the steel substrate. Hence, the introduction of the 15 g/L $ZnSO_4$ in the electroless Ni-P bath results in the deposition of a sacrificial coating that provides better corrosion protection to steel substrates.

Conclusions

Composite Ni-Zn-P alloys with different amounts of Zn were prepared by controlling the amount of Zn^{2+} ions added in the bath. Material characterization studies on the resultant coatings showed the codeposition of Zn along with Ni and P. The Zn content in the alloy can be controlled by varying the Zn^{2+} concentration in the bath or by adjusting the bath pH. Increasing the temperature of the bath increases the deposition rate. Material and electrochemical characterization studies reveal that composites with 16.2 wt % Zn show a potential that is more electronegative to steel and hence is applicable as a sacrificial coating for the protection of steel. This optimal Zn content in the alloy is obtained when deposition is carried out with a $ZnSO_4$ concentration of 15 g/L at pH 10.5 and 85°C. The high Ni content (74.0 wt %) ensures the superior corrosion resistance of the composite alloy as compared to conventional Zn-based coatings obtained by electrolysis. Polarization resistance studies reveal a four-time increase in the resistance value for the Ni-Zn-P coating over that of Cd. Finally, the low potential difference that exists between the coating and the substrate results in a lower dissolution rate for the deposited alloy as compared to Zn, Zn-Ni and Cd coatings.

Acknowledgments

Financial support by Dr. Vinod Agarvala, The Office of Naval Research, under grant no. NOOOO14-00-1-0053 and AESF research contract, project 107, are gratefully acknowledged. This work was also partially supported by Sandia National Laboratories. Sandia is a

multiprogram laboratory operated by Sandia Corporation, a Lockheed Martin Company, for the United States Department of Energy under contract DE-AC-4-94-AL85000.

University of South Carolina assisted in meeting the publication costs of this article.

Appendix

The electroless bath used for deposition consists of 35 g/L $NiSO_4 \cdot 6H_2O$, 15 g/L $ZnSO_4 \cdot 7H_2O$, 85 g/L Sodium citrate and 50 g/L Ammonium chloride. The variables to be determined are as follows: $[Zn^{2+}]$, $[Ni^{2+}]$, $[Zn(OH)^+]$, $[Ni(OH)^+]$, $[Zn(OH)_2]$, $[Ni(OH)_2]$, $[Zn(NH_3)_4^{2+}]$, $[Ni(NH_3)_6^{2+}]$, $[Zn_2(OH)^{3+}]$, $[OH^-]$, $[SO_4^{2-}]$, and $[HSO_4^-]$. The concentration of $[H^+]$ depends on the specified pH. The equations used for the determination of the equilibrium concentrations are

Material balance on zinc

$$[ZnSO_4]_{ad} = [Zn^{2+}] + [Zn(OH)^+] + 2[Zn_2(OH)^{3+}] + [Zn(OH)_2] + [Zn(NH_3)_4^{2+}]$$

Material balance on nickel

$$[NiSO_4]_{ad} = [Ni^{2+}] + [Ni(OH)^+] + [Ni(OH)_2] + [Ni(NH_3)_6^{2+}]$$

Electroneutrality conditions

$$[H^+] + 2[Zn^{2+}] + 2[Ni^{2+}] + [Zn(OH)^+] + [Ni(OH)^+] + 3[Zn_2(OH)^{3+}] + 2[Zn(NH_3)_4^{2+}] + 2[Ni(NH_3)_6^{2+}] = [HSO_4^-] + [SO_4^{2-}] + [OH^-]$$

The equilibrium conditions

$$[H^+][SO_4^{2-}] - k_1[HSO_4^-] = 0$$

$$[Zn^{2+}][OH^-] - k_2[Zn(OH)^+] = 0$$

$$[Ni^{2+}][OH^-] - k_3[Ni(OH)^+] = 0$$

$$[H^+][OH^-] - k_4 = 0$$

$$[Zn^{2+}]^2[OH^-] - k_5[Zn_2(OH)^{3+}] = 0$$

$$[Zn(OH)^+][OH^-] - k_6 = 0$$

$$[Ni(OH)^+][OH^-] - k_7 = 0$$

$$[Zn(OH)_2][NH_3]_{ad}^4 - k_8[Zn(NH_3)_4^{2+}][OH^-]^2 = 0$$

$$[Ni(OH)_2][NH_3]_{ad}^6 - k_9[Zn(NH_3)_6^{2+}][OH^-]^2 = 0$$

The above equations were solved simultaneously by using Maple.® The various rate constants used in the equations are as follows: $k_1 = 1.2 \times 10^{-2}$ mol/L, $k_2 = 1.1 \times 10^{-6}$ mol/L, $k_3 = 2.0 \times 10^{-5}$ mol/L, $k_4 = 1.0 \times 10^{-14}$ mol^2/L^2, $k_5 = 5.1622 \times 10^{-8}$ mol^2/L^2, $k_6 = 1.3 \times 10^{-16}$ mol^2/L^2, $k_7 = 6.3 \times 10^{-16}$ mol^2/L^2, $k_8 = 2.1 \times 10^7$ mol^2/L^2, and $k_9 = 1.7 \times 10^6$ mol^2/L^2.

References

1. K. R. Baldwin and C. J. E. Smith, *Trans. Inst. Met. Finish.*, **74**, 202 (1996).
2. W. H. Safranek, *Plat. Surf. Finish.*, **85**, 45 (1997).
3. A. Ashur, J. Sharon, and I. E. Klein, *Plat. Surf. Finish.*, **83**, 58 (1996).
4. S. Swathirajan, *J. Electrochem. Soc.*, **133**, 671 (1986).
5. N. R. Short, S. Zhou, and J. K. Bennis, *Surf. Coat. Technol.*, **79**, 218 (1996).
6. Y. P. Lin and J. R. Selman, *J. Electrochem. Soc.*, **140**, 1299 (1993).
7. A. Shibuya, T. Kurimoto, K. Korekewa, and K. Noti, *Tetsu to Hagane*, **66**, 71 (1980).
8. A. Brenner, *Electrodeposition of Alloys, Principles and Practice*, Chap. 1, Academic Press, New York (1963).
9. N. S. Grigoryan, V. N. Kudryavtsev, P. A. Zhdan, I. Y. Kolotyrkin, E. A. Volynskaya, and T. A. Vagramyan, *Zasch. Met.*, **25**, 288 (1989).
10. B. N. Popov, D. Slavkov, T. Grecv, Lj. Arsov, and S. Kariavanov, *Kem. Ind.*, **1**, 1 (1986).
11. Z. Zhou and T. J. O. Keefe, *Surf. Coat. Technol.*, **96**, 191 (1997).
12. A. Krishniyer, M. Ramasubramanian, B. N. Popov, and R. E. White, *Plat. Surf. Finish.*, **87**, 99 (1999).
13. A. Durairajan, A. Krishniyer, B. N. Popov, B. Haran, and S. N. Popova, *Corrosion (Houston)*, **56**, 283 (2000).
14. A. Durairajan, B. S. Haran, R. E. White, and B. N. Popov, *J. Electrochem. Soc.*, **147**, 1781 (2000).
15. M. Bouanani, F. Cherkaoui, R. Fratesi, G. Roventi, and G. Barucca, *J. Appl. Electrochem.*, **29**, 637 (1999).
16. E. Valova, I. Georgiev, S. Armyanov, J.-L. Delplancke, D. Tachev, Ts. Tsacheva, and J. Dille, *J. Electrochem. Soc.*, **148**, C266 (2001).
17. M. Schlesinger, X. Meng, and D. D. Snyder, *J. Electrochem. Soc.*, **138**, 406 (1991).
18. *Standard Practice for Measuring Thickness of Electrodeposited and Related Coatings*, Vol. 02-05, Desg. B659, ASTM Standards, ASTM.
19. I. Ohno, *Mater. Sci. Eng., A*, **146**, 33 (1991).
20. J. R. Carbajal and R. E. White, *J. Electrochem. Soc.*, **135**, 2952 (1988).
21. W. M. Latimer, *Oxidation States of the Elements and Their Potentials in Aqueous Solutions*, Prentice-Hall Inc., New York (1952).
22. G. Roventi, R. Fratesi, R. A. Della Guardia, and G. Abrucca, *J. Appl. Electrochem.*, **30**, 173 (2000).
23. F. J. Fabri Miranda, O. E. Barcia, O. R. Mattas, and R. Wiart, *J. Electrochem. Soc.*, **144**, 3449 (1997).
24. J. Leukonis, *Zh. Prikl. Khim. (S.-Peterburg)*, **51(8)**, 1797 (1978).
25. M. Ratzker, D. S. Lashmore, and K. W. Pratt, *Plat. Surf. Finish.*, **73(9)**, 74 (1986).
26. M. Pourbaix, *Atlas of Electrochemical Equilibria in Aqueous Solutions*, Permagon Press, New York (1966).
27. F. J. Fabri Miranda, I. C. P. Margarit, O. R. Mattos, O. E. Barcia, and R. Wiart, *Corrosion (Houston)*, **55(8)**, 732 (1999).